

Predicting Human Eye Fixations via an LSTM-based Saliency Attentive Model

Marcella Cornia Lorenzo Baraldi Giuseppe Serra Rita Cucchiara
 University of Modena and Reggio Emilia
 name.surname@unimore.it

Abstract

Data-driven saliency has recently gained a lot of attention thanks to the use of Convolutional Neural Networks. In this paper we go beyond the standard approach to saliency prediction, in which gaze maps are computed with a feed-forward network, and we present a novel Saliency Attentive Model which can predict accurate saliency maps by incorporating attentive mechanisms. Our solution is composed of a Convolutional LSTM, that iteratively focuses on the most salient regions of the input, and a Residual Architecture designed to preserve spatial resolution. Additionally, to tackle the center bias present in human eye fixations, our model incorporates prior maps generated by learned Gaussian functions. We show, through an extensive evaluation, that the proposed architecture overcomes the current state of the art on three public saliency prediction datasets: SALICON, MIT300 and CAT2000. We further study the contribution of each key components to demonstrate their robustness on different scenarios.

1. Introduction

Visual cognition science has shown that when humans observe a scene, they do not focus on each part with the same intensity. Instead, attentive mechanisms guide their gazes on salient and relevant regions, focusing on different elements of the scene such as bright colors, texts, faces or sudden movements [41]. An intensive research effort from the computer vision community has focused on emulating such selective visual mechanisms, as computational saliency models can be applied to a wide range of applications such as image retargeting [8, 44], object recognition [52], video compression [15] and visual tracking [38].

Traditional saliency prediction methods have followed biological evidences by defining features that capture low-level cues such as color, contrast and texture or semantic concepts such as faces, people and text [16, 14, 26, 58]. However, these techniques fail to capture the wide variety of possible causes that contribute to define visual saliency maps.

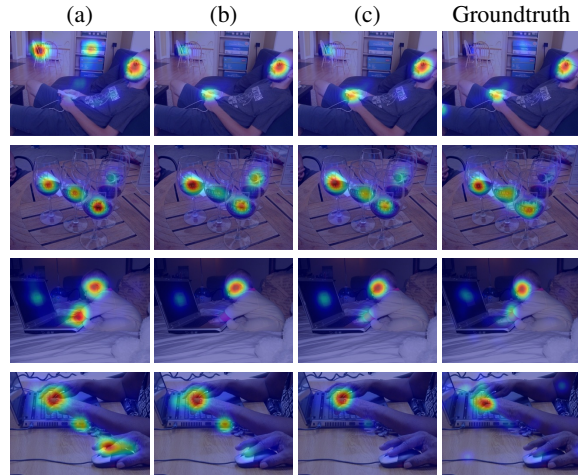


Figure 1: Our saliency prediction model is composed by three main parts: a Dilated Residual Convolutional Network (DRCN), an Attentive Convolutional LSTM and a set of learnable priors. We show some examples of saliency maps predicted by the DRCN (a), the DRCN with Attentive ConvLSTM (b), and the DRCN with Attentive ConvLSTM and learned priors (c).

Since 2014, with the advent of deep neural networks, researchers have investigated several convolutional architectures for addressing this task [51, 32, 20, 30, 23, 10]. Although these approaches allowed researchers to include specific saliency loss functions [20] or global context information [30], no one has yet investigated the incorporation of attention mechanisms in saliency prediction. Attentive models, indeed, can infer relevant parts of an image by selectively focusing on different regions of the scene; they have achieved state of the art results in several contexts such as image captioning [55], machine translation [9] and action recognition [35].

In this paper we investigate the usage of attentive models in saliency prediction. In particular, we propose a novel end-to-end saliency prediction architecture that incorporates an Attentive Convolutional Long Short-Term Memory network (Attentive ConvLSTM) that iteratively infers rele-

vant salient regions of the scene. For the first layers of our solution, differently from all the previous approaches based on classical Convolutional Neural Networks (CNNs), we propose a new Residual Neural Network [18] specifically designed to maintain spatial resolution; we call it Dilated Residual Neural Network (DRCN). This residual architecture, which reduces the downscaling effect, allows us to obtain improved feature extraction capabilities with respect to classical CNNs.

Moreover, to handle the tendency of humans to fix the center region of an image, we introduce an explicit center prior component. Unlike recent approaches that include handcrafted center priors [26, 30, 32, 33, 51], we present a module that keeps the architecture trainable end-to-end and which is able to learn priors automatically. We call the overall architecture Saliency Attentive Model (SAM). Figure 1 shows examples of saliency predictions obtained by using the full proposed solution and the architectures based on the main components.

We quantitatively validate our approach on three publicly available benchmark datasets: SALICON, MIT300 and CAT2000. Experimental results show that the proposed solution achieves state of the art performances and that the incorporation of an attentive architecture can significantly improve prediction. In addition, both our DRCN and the learned priors strategy increase the overall performance.

To sum up, our contributions are threefold:

- We propose a new Attentive ConvLSTM that sequentially refines predicted saliency maps. To the best of our knowledge, this is the first attempt to incorporate attentive models in a saliency prediction architecture.
- We include in our architecture a Dilated Residual Convolutional Network that extracts features from input images limiting the rescaling of saliency maps. Furthermore, our network is able to learn the center bias present in eye fixations, differently from other previous models that integrate this information manually.
- The proposed solution overcomes by a big margin the current state of the art on the largest dataset available for the saliency prediction task, the SALICON dataset. Moreover, on MIT300 and CAT2000 datasets our method achieves state of the art results showing good generalization properties.

2. Related Work

Preliminary works on saliency prediction were based on the Feature Integration Theory proposed by Treisman *et al.* [48] in the eighties. Itti *et al.* [22] proposed the first computational model to predict saliency on images: this work, inspired by Koch and Ullman [28], computed a set of individual topographical maps representing low-level cues such

as color, intensity and orientation and combined them into a global saliency map. After this work, a large variety of methods explored the same idea of combining complementary low-level features [4, 16, 50, 12] and often included additional center-surround cues [39, 58]. Other methods enriched predictions exploiting semantic classifiers for detecting higher level concepts such as faces, persons, cars and horizons [7, 26, 59, 14, 1].

In the last few years, thanks to the large spread of deep learning techniques, the saliency prediction task has achieved a considerable improvement. A first attempt to predict saliency with convolutional networks has been performed by Vig *et al.* [51] who proposed the *Ensemble of Deep Networks (eDN)* model. This model consists of three convolutional layers followed by a linear classifier, trained on salient and non-salient regions, that blend feature maps coming from the previous layers. This method inspired Kümmerer *et al.* [32] who proposed a new deep saliency prediction model built upon the well known Krizhevsky’s architecture (AlexNet) [29]. This method, called *DeepGaze I*, maintains the AlexNet parameters fixed and a linear combination of feature maps coming from the previous network is fed through a softmax rectification to yield a two dimensional probability distribution. Recently, a second version of this work, *DeepGaze II* [33], was presented and, instead of using the AlexNet model, it employs the VGG19 network [45] achieving improved performance.

These models mainly suffered from the absence of fine-tuning of network parameters over a saliency prediction dataset. Liu *et al.* [37], for this reason, presented a multiresolution convolutional neural network (*Mr-CNN*) trained over image patches centered on fixation and non-fixation locations. This method maintained state of the art results until the publication of large-scale attention datasets, such as SALICON [24], which have contributed to a big progress of deep saliency prediction models.

Huang *et al.* [20] introduced an architecture consisting in a deep neural network applied at two different image scales. They also used some evaluation metrics specific for the saliency prediction task (such as KL-Divergence, Normalized Scanpath Saliency, Linear Correlation Coefficient and Similarity) as loss functions. Kruthiventi *et al.* [30] proposed a fully convolutional network called *DeepFix* that captures features at multiple scales and takes global context into account through the use of large receptive fields. Moreover, *DeepFix* takes advantage of predefined priors to predict its saliency maps, getting a large improvement from using them. Pan *et al.* [40] instead presented a shallow and a deep convnet where the first is trained from scratch while some layers of the second are initialized with the VGG parameters.

Jetley *et al.* [23] introduced a saliency map model that formulates a map as a generalized Bernoulli distribution and

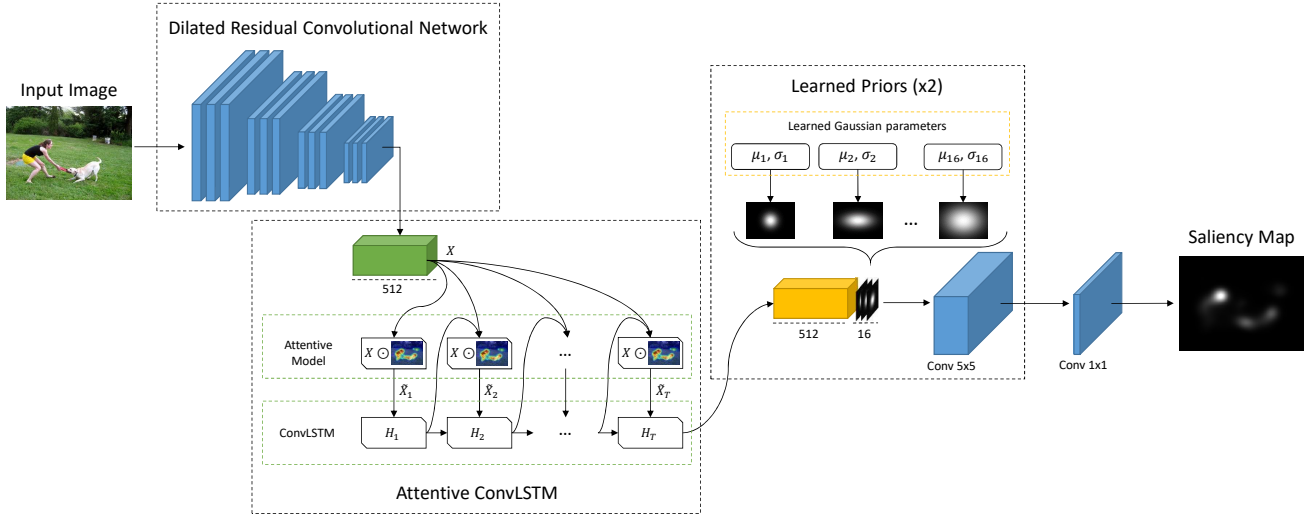


Figure 2: Overview of our Saliency Attentive Model (SAM).

they used these maps to train a deep network trying different loss functions. Kruthiventi *et al.* [31] instead presented a unified framework that is capable of predicting eye fixations and segmenting salient objects on input images. Finally, Cornia *et al.* [10] proposed a new deep architecture (called *ML-Net*) based on the VGG16 model, that uses feature maps coming from multiple levels of the VGG network.

For the sake of clarity, the saliency prediction task is strictly related to that of salient object detection, even though they are significantly different. Salient object detection consists, indeed, in identifying a binary map indicating the presence of salient objects [34, 53, 57, 60]. In this work, we are interested in predicting eye fixations from an input image employing a new saliency attentive model.

3. Model Architecture

Our model leverages three main contributions. Firstly, instead of employing a classical CNN to process the input image [20, 30, 40, 10], we build a residual architecture which shows better feature learning capabilities, while at the same time limiting downscaling effects which can worsen saliency prediction performance, as we demonstrate in our experiments. Then, we propose an Attentive Convolutional model, which recurrently refines the saliency map by selectively attending to different spatial regions. Predictions are finally combined with multiple learned priors. A summary of the overall architecture of our model is shown in Figure 2.

3.1. Dilated Residual Convolutional Network

The first component of the model is a fully convolutional network that extracts feature maps from the input image using residual connections [18]. Instead of having a series

of stacked layers that process the input image as in common CNNs, a residual network performs a series of residual mappings between blocks composed by a few stacked layers. This is obtained using shortcut connections that realize an identity mapping, *i.e.* the input of the block is added to its output. Residual connections help to avoid the accuracy degradation problem [17] that occurs with the increase of the network depth, and show to be beneficial also in the saliency prediction case, since they improve the feature extraction capabilities of the network.

Our residual network is inspired by the recent ResNet-50 model [18] that consists of five convolutional blocks and a fully connected layer. Since the purpose of our network is to extract feature maps, we only consider convolutional layers and ignore the fully connected layer. The first block is composed by one convolutional layer followed by a max-pooling layer, both of them having a stride of 2, while the remaining four blocks are fully convolutional. In the standard ResNet-50 model, all of these blocks, except `conv2`, reduce the dimension of feature maps with strides of 2. The overall architecture of the ResNet-50 network is reported in Figure 3a.

It can be noticed that the downscaling factor of this architecture is particularly critical. For example, with an input image having a size of 270×360 , the output dimension is 9×12 , which is relatively small for the saliency prediction task. For this reason, we modify the network structure to limit the rescaling phenomena. In the last two blocks, we remove the stride to preserve the output dimensions and we introduce dilated convolutions [56]. These ensure that filters of the final blocks operate on the same receptive field for which they were originally conceived, and that pre-trained weights can be properly fine-tuned. In par-

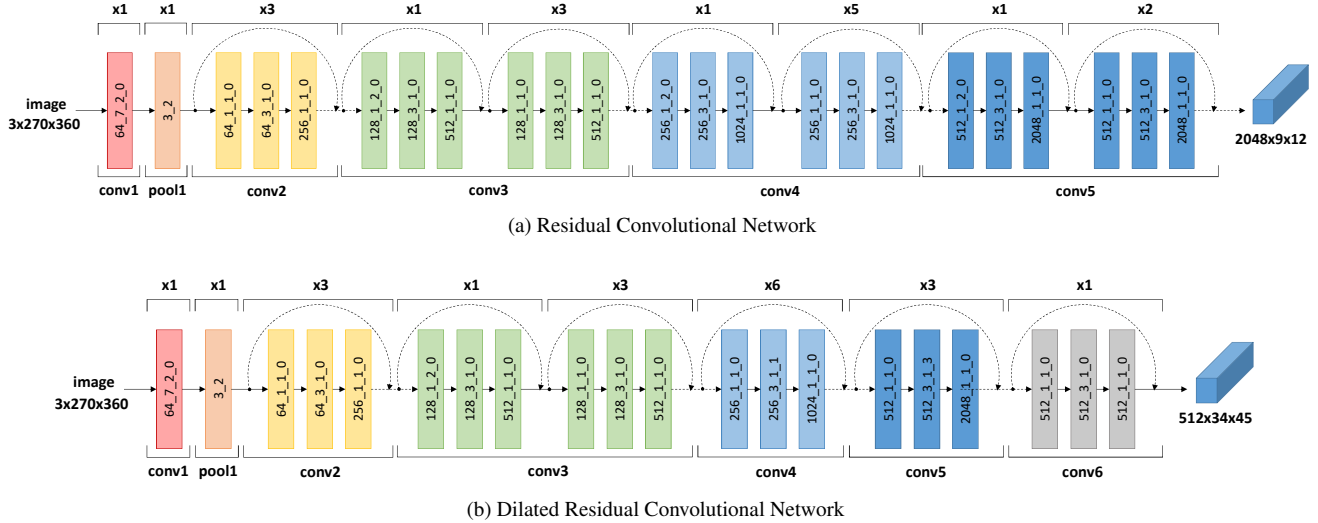


Figure 3: Overall architectures of the residual convolutional network with and without dilated convolutions. Convolutional and pooling blocks are respectively expressed in terms of [channels_kernel_stride_holes] \times repetitions and [kernel_stride] \times repetitions.

ticular, we introduce holes of size 1 in the kernels of the block `conv4` and holes of size $2^2 - 1 = 3$ in the kernels of the block `conv5`.

The use of dilated convolutions allows the layer to have a larger receptive field without increasing the number of parameters. In fact, visual saliency is the distinct perceptual quality which makes some items in an observed scene stand out from their neighbors [21]. Thanks to these expedients, our saliency maps are rescaled by a factor of 8 instead of 32 as in the original ResNet-50.

The output of the residual network is a tensor with 2048 channels. To limit the number of feature maps, we fed this tensor into another convolutional block, which is composed by three convolutional layers with 512 filters, followed by a shortcut connection. Notice that we employ a residual structure also for this block, to preserve a residual nature within the entire feature extraction architecture. The kernel size of the first and the last layer is set to 1, while the kernel size of the second layer is set to 3. The overall architecture of the Dilated Residual Convolutional Network is reported in Figure 3b.

3.2. Attentive Convolutional LSTM

Having computed a set of feature maps for the input image, we propose an Attentive Convolutional LSTM which sequentially refines feature maps thanks to an attentive recurrent mechanism.

Although LSTM networks [19] have achieved good performances on tasks like action recognition [11], image captioning [27] and visual question answering [54], they can not be directly employed for saliency prediction, as they

work on sequences of vectors. For this reason, we extend the traditional LSTM to work on images by substituting dot products with convolutional operations.

Our attentive model takes as input a stack of features extracted from the input image, which are sequentially processed to produce a refined stack of feature maps. Specifically, our LSTM is updated according to the following equations

$$I_t = \sigma(W_i * \tilde{X}_t + U_i * H_{t-1} + b_i) \quad (1)$$

$$F_t = \sigma(W_f * \tilde{X}_t + U_f * H_{t-1} + b_f) \quad (2)$$

$$O_t = \sigma(W_o * \tilde{X}_t + U_o * H_{t-1} + b_o) \quad (3)$$

$$G_t = \tanh(W_c * \tilde{X}_t + U_c * H_{t-1} + b_c) \quad (4)$$

$$C_t = F_t \odot C_{t-1} + I_t \odot G_t \quad (5)$$

$$H_t = O_t \odot \tanh(C_t) \quad (6)$$

here, $*$ represents the convolutional operator, all W and U are 2-d convolutional kernels, and all b are learned biases. The gates I_t , F_t , O_t , the candidate memory G_t , memory cell C_t , C_{t-1} , and hidden state H_t , H_{t-1} are 3-d tensors, each of them having 512 channels.

The input of the LSTM layer \tilde{X}_t is computed, at each timestep, through an attentive mechanism which selectively focuses on different regions of the input feature stack. In particular, the LSTM computes an attention map which is generated by convolving the previous hidden state H_{t-1} and the input X , feeding the result to a \tanh activation function and finally convolving with a one channel convolutional kernel

$$Z_t = V_a * \tanh(W_a * X + U_a * H_{t-1} + b_a). \quad (7)$$

The output of this operations is a 2-d map from which we can compute a normalized spatial attention map

$$A_t^{ij} = p(att_{ij}|X, H_{t-1}) = \frac{\exp(Z_t^{ij})}{\sum_i \sum_j \exp(Z_t^{ij})} \quad (8)$$

where A_t^{ij} is the element of the attention map in position (i, j) . The attention map is applied to the input X with an element-wise product between each channel of the feature maps and the attention map

$$\tilde{X}_t = A_t \odot X. \quad (9)$$

This way, the attention map inhibits the activations from the spatial locations that have lower attention saliency.

3.3. Learned Priors

Psychological studies have shown that when observers look at images, their gazes are biased toward the center [46, 49]. To take this bias into account, several saliency approaches have incorporated handcrafted center priors [26, 30, 32, 33, 51]. Although these solutions have proven to be effective, identifying optimal prior maps for all possible scenarios is not trivial. To address this issue, we integrate a module which can learn prior maps from data, keeping the architecture trainable end-to-end.

We model the center bias by means of a set of Gaussian functions with diagonal covariance matrix. Means and variances are learned for each prior map, according to the following equation:

$$f(x, y) = \frac{1}{2\pi\sigma_x\sigma_y} \exp\left(-\left(\frac{(x-\mu_x)^2}{2\sigma_x^2} + \frac{(y-\mu_y)^2}{2\sigma_y^2}\right)\right). \quad (10)$$

Our network learns the parameters of N Gaussian functions (in our experiments $N = 16$) and generates the relative prior maps. These maps are then concatenated with the output tensor of the Attentive ConvLSTM. Since this tensor has 512 channels, after the concatenation with learned prior maps, we obtain a tensor with 528 channels. The resulting tensor is fed through another convolutional block to maintain the residual structure of our network.

We include dilated convolution also in this block thus obtaining a convolutional layer with a large receptive field that allows us to capture the saliency of an object with respect to its neighborhood. We set the kernel size of this layer to 5 and the holes size to 3 achieving therefore a receptive field of 17×17 . This module is replicated two times.

The last layer of our model is a convolutional operation with one filter and a kernel size of 1 that extracts the final saliency map.

4. Experimental Evaluation

In this section we perform an analysis concerning the contribution of each component of our network and a quan-

titative and qualitative comparison with other state of the art models. First, we describe datasets and metrics used to evaluate our saliency prediction model and provide implementation details.

4.1. Datasets and Metrics

Four of the most popular saliency datasets are considered for evaluation, and quantitative experiments are carried out by using a variety of different metrics.

SALICON [24] This is the largest dataset currently available for saliency prediction and it contains 10,000 training images, 5,000 validation images and 5,000 testing images, all taken from the Microsoft CoCo dataset [36]. In this dataset, eye fixations are simulated with mouse movements instead of using eye-tracking systems. Authors of [24] show an high degree of similarity between their mouse-contingent saliency annotations and those recorded with an eye-tracking system. The groundtruth maps of the testing set are not publicly available, therefore, to evaluate the effectiveness of our model, we submitted our predicted saliency maps to the SALICON challenge website.

MIT1003 [26] The MIT1003 dataset contains 1003 images coming from Flickr and LabelMe. Saliency maps have been created from eye-tracking data of 15 observers.

MIT300 [25] The MIT300 dataset is a collection of 300 natural images where saliency maps were generated from eye-tracking data of 39 users. Saliency maps of this entire dataset are held out and we used the MIT Saliency benchmark [5] for evaluating our predictions.

CAT2000 [2] This dataset contains 4,000 images coming from a large variety of categories such as *Cartoons, Art, Satellite, Low resolution images, Indoor, Outdoor, Line drawings*, ect. It is composed by 20 different categories with 200 images for each of them. Saliency maps of the testing set, composed by 2,000 images, are not available and also in this case we submitted our predicted saliency maps to the MIT Saliency benchmark [5].

Metrics There exists a large variety of metrics to evaluate the effectiveness of saliency prediction models and the main difference between them concerns the ground-truth representation. In fact, saliency evaluation metrics can be categorized in location-based and distribution-based metrics [42, 6]. The first category considers saliency maps at discrete fixation locations, while the second treats both ground-truth fixation maps and predicted saliency maps as continuous distributions.

The most widely used location-based metrics are the Area under the ROC curve, in its different variants of Judd (AUC) and shuffled (sAUC), and the Normalized Scanpath Saliency (NSS). The AUC metrics do not penalize low-valued false positives giving an high score for high-valued predictions placed at fixated locations and ignoring the others. Besides, the sAUC is designed to penalize models that

take into account the center bias present in eye fixations. The NSS, instead, is sensitive in an equivalent manner to both false positives and false negatives.

For the distribution-based category, the most used evaluation metrics are the Linear Correlation Coefficient (CC), the Similarity (SIM) and the Earth Mover Distance (EMD). The CC treats both false positives and false negatives symmetrically, differently from the SIM that instead measures the intersection between two distributions and for this reason it is very sensitive to missing values. The EMD is a dissimilarity metric that penalizes false positives proportionally to the spatial distance from the groundtruth.

4.2. Implementation Details

4.2.1 Preprocessing

We evaluate our model on SALICON, MIT300 and CAT2000 datasets. For the first dataset, we train the network on its training set and we use the 5,000 validation images to validate the model. For the second and the third dataset, we fine-tune our network, trained on SALICON, on the MIT1003 dataset and on the CAT2000 training set respectively as suggested by the MIT Saliency benchmark organizers. In particular, we use 903 randomly selected images of the MIT1003 to fine-tune our network and the other 100 as validation set. For the CAT2000 dataset, instead, we randomly choose 1,800 images of training set for the fine-tuning and we use the remaining 200 (10 for each category) as validation set.

All input images are resized to 270×360 . Images from MIT1003 and MIT300 datasets are zero padded to have an aspect ratio of 4:3 and then resized to have the selected input size. Images from CAT2000 dataset, instead, are cropped and then resized.

4.2.2 Training

At training time, we randomly sample a minibatch containing K training saliency maps (in our experiments $K = 10$), and encourage the network to minimize a loss function through the RMSprop optimizer [47].

Weights of the residual network are initialized with those of the ResNet-50 model trained on ImageNet [43]. For the Attentive ConvLSTM, we initialize the recurrent weights matrices U_i , U_f , U_o and U_c as random orthogonal matrices. All W matrices and U_a are initialized by sampling each element from the Gaussian distribution of mean 0 and variance 0.05^2 . The matrix V_a and all bias vectors are initialized to zero. Weights of all other convolutional layers of our model are initialized according to [13].

We test four different loss functions: the KL-Divergence (KL-Div), the Linear Correlation Coefficient (CC), the Euclidean Loss and the square error loss used in [10] (ML-Net

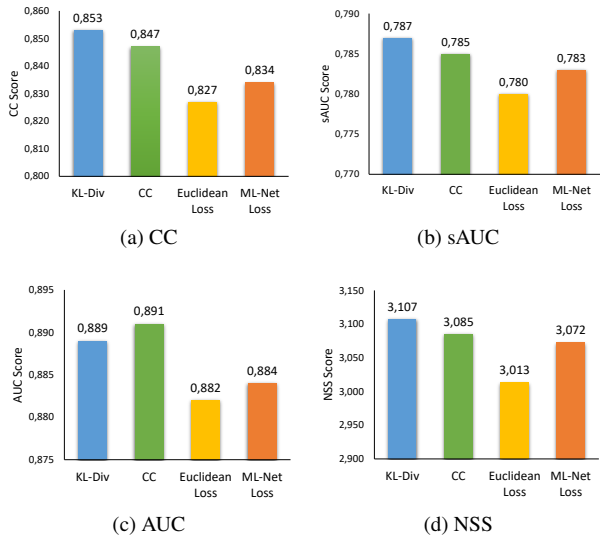


Figure 4: Comparison between different loss functions on SALICON validation set [24]. Each plot corresponds to a different evaluation metric (CC, sAUC, AUC and NSS). The four color bars represent the performance of the proposed network trained with the considered loss functions.

Loss). Figure 4 shows the results of our model when using the considered loss functions to train the network on the SALICON validation set. As it can be observed, the KL-Divergence achieves the best performance, overcoming the other losses on all considered metrics except for the AUC. Following these findings, results in the next subsections are obtained by training the network with KL-Divergence. With these experimental settings, we set the initial learning rate to 10^{-4} and we decrease it by a factor of 10 every two epochs.

4.3. Results

4.3.1 Model Ablation Analysis

We evaluate the contribution of each component of the proposed model on SALICON, MIT1003 and CAT2000 validation sets. To this end, we construct four different variations of our model: the plain ResNet-50 architecture without the last fully convolutional layer, our Dilated Residual Convolutional Network (DRCN), the DRCN with the proposed attentive model and the final version of our model with all its components.

Table 1 shows the results of the ablation analysis on the considered datasets. The results empathize that the overall architecture is able to predict better saliency maps on all datasets and each of proposed component gives an important contribution to the final performances. In particular, on the SALICON dataset, it can be seen that there is a constant improvement on all metrics. For example, the ResNet-50

	SALICON				MIT1003				CAT2000			
	CC	sAUC	AUC	NSS	CC	sAUC	AUC	NSS	CC	sAUC	AUC	NSS
ResNet-50	0.769	0.760	0.872	2.515	0.649	0.674	0.891	2.272	0.866	0.636	0.872	2.244
DRCN	0.811	0.775	0.883	2.928	0.722	0.675	0.906	2.658	0.877	0.637	0.873	2.317
DRCN + Attentive LSTM	0.847	0.785	0.887	3.091	0.764	0.680	0.914	2.878	0.888	0.637	0.875	2.372
DRCN + Att. LSTM + Priors	0.853	0.787	0.889	3.107	0.768	0.685	0.913	2.846	0.892	0.639	0.876	2.370

Table 1: Model ablation analysis on SALICON [24], MIT1003 [26] and CAT2000 [2] validation sets.

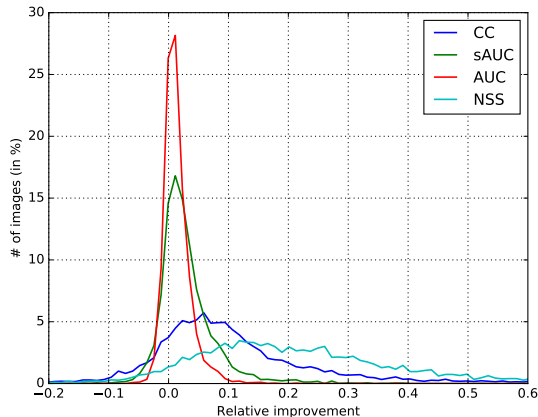


Figure 5: The graph shows the relative improvement achieved by the proposed solution on the SALICON validation set in terms of numbers of images (expressed in %). The improvement is measured with respect to the ResNet-50 model and it is calculated on CC, sAUC, AUC and NSS metrics. Best viewed in color.

baseline achieves a result of 0.769 in terms of CC, while the DRCN achieves an improvement of $\frac{0.811-0.769}{0.769} = 5.5\%$. This result is further improved by a 4.4% when adding the Attentive ConvLSTM; finally, the learned priors add another slight improvement of 0.7%.

Also on MIT1003 and CAT2000 datasets, the proposed Attentive ConvLSTM and the DRCN achieve a big enhancement to the overall results while the contribution of learned priors is less evident.

To further examine the contribution of the proposed model with respect to the ResNet-50 baseline, we compute the relative improvement on each image, in terms of CC, sAUC, AUC, and NSS. Figure 5 shows the distribution of the per-image relative improvement, computed on SALICON validation set. As it can be noticed, the final model achieves the most consistent improvements on the CC and NSS metrics. Since these metrics, differently from the AUC, penalize equally both false positive and false negative, it means our complete solution is able to predict more accurate saliency maps than the ResNet-50, without intro-

	CC	sAUC	AUC	NSS
Shallow [40]	0.562	0.670	0.836	1.663
DeepGazeII [33]	0.509	0.761	0.885	1.336
SalNet [40]	0.622	0.724	0.858	1.859
ML-Net [10]	0.743	0.768	0.866	2.789
PDP [23]	0.765	0.781	0.882	-
SU [31]	0.780	0.760	0.880	2.610
Our method	0.851	0.778	0.887	3.058

Table 2: Comparison results on SALICON test set [24]. The method in [23] does not provide the NSS value. The results in bold indicate the best performing method on each evaluation metric.

ducing additional blurred regions.

4.3.2 Comparison with state of the art

We quantitative compare our method with recent and relevant state of the art models on SALICON, MIT300 and CAT2000 test sets.

Table 2 shows the results on the SALICON dataset in terms of CC, sAUC, AUC and NSS. As it can be observed, our solution outperforms all competitors by a big margin especially on CC and NSS metrics and obtains the best result also on the AUC. In detail, our method overcomes all other recent models with an improvement of 9% according to CC metric, 0.2% and 10% according to AUC and NSS.

The results on MIT300 and CAT2000 datasets are respectively reported in Tables 3 and 4. Our method achieves state of the art results on both datasets in terms of SIM, CC and NSS and good results on AUC and EMD overcoming all other models on the CAT2000 dataset. The proposed solution does not obtain a big gain in performance especially on the AUC metrics. This can be explained considering that the AUC metrics are primarily based on true positives without significantly penalizing false positives. For this reason, hazy or blurred saliency maps achieve high AUC values [3, 59]. Furthermore, since our model incorporates learned priors, we obtain lower sAUC values de-

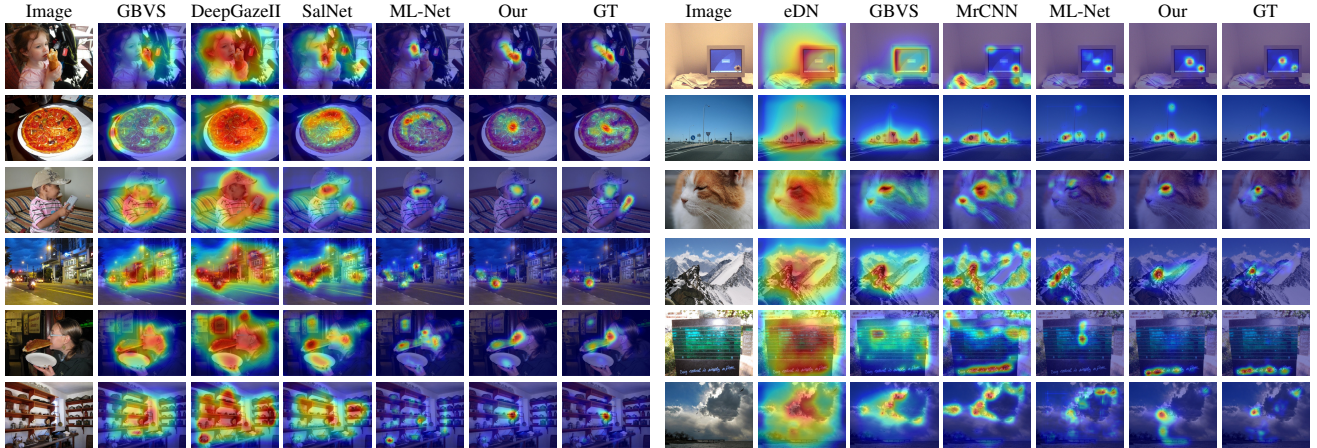


Figure 6: Qualitative results and comparison with other state of the art models. Left images are from SALICON validation set [24], while right images are from MIT1003 validation set [26].

	SIM	CC	sAUC	AUC	NSS	EMD
eDN [51]	0.41	0.45	0.62	0.82	1.14	4.56
Judd [26]	0.42	0.47	0.60	0.81	1.18	4.45
GBVS [16]	0.48	0.48	0.63	0.81	1.24	3.51
Mr-CNN [37]	0.48	0.48	0.69	0.79	1.37	3.71
BMS [58]	0.51	0.55	0.65	0.83	1.41	3.35
SalNet [40]	0.52	0.58	0.69	0.83	1.51	3.31
DeepGazeII [33]	0.46	0.52	0.72	0.88	1.29	3.98
ML-Net [10]	0.59	0.67	0.70	0.85	2.05	2.63
PDP [23]	0.60	0.70	0.73	0.85	2.05	2.58
SALICON [20]	0.60	0.74	0.74	0.87	2.12	2.62
DeepFix [30]	0.67	0.78	0.71	0.87	2.26	2.04
Our method	0.67	0.79	0.71	0.87	2.31	2.06

Table 3: Comparison results on the MIT300 dataset [25]. The results in bold indicate the best performing method on each evaluation metric.

spite our saliency maps are visually more similar with the groundtruth ones.

Qualitative results obtained by our model on SALICON and MIT1003 validations sets, with that of some other state of the art models, are shown in Figure 6. As it can be noticed, our network is able to predict high saliency values on faces, texts and other predominant cues. Furthermore, our model is capable, not only of predicting the saliency on people faces, but also on the objects with which they interact. Other examples show that the proposed solution produces good saliency maps also when images do not contain significant salient regions (for example when the saliency is

	SIM	CC	sAUC	AUC	NSS	EMD
Judd [26]	0.46	0.54	0.56	0.84	1.30	3.60
GBVS [16]	0.51	0.50	0.58	0.80	1.23	2.99
eDN [51]	0.52	0.54	0.55	0.85	1.30	2.64
BMS [58]	0.61	0.67	0.59	0.85	1.67	1.95
DeepFix [30]	0.74	0.87	0.58	0.87	2.28	1.15
Our method	0.77	0.90	0.58	0.88	2.40	1.06

Table 4: Comparison results on the CAT2000 test set [2]. The results in bold indicate the best performing method on each evaluation metric.

concentrated in the center of the scene or when images portray a landscape).

5. Conclusion

We proposed a new Saliency Attentive Model that predicts human eye fixations on natural images. The proposed solution is composed by an Attentive Convolutional LSTM that is specifically designed to sequentially focus on the most salient regions of input images. Furthermore, we included a residual architecture that maintains spatial resolution, and learned priors that are able to model the center bias present in the saliency maps. We demonstrated the effectiveness of each component with an extensive evaluation on three of the most important datasets, and we showed our model achieves state of the art results.

Acknowledgement

This work was partially supported by the Fondazione Cassa di Risparmio di Modena project: “Vision for Aug-

mented Experience”. We acknowledge the CINECA award under the ISCRA initiative, for the availability of high performance computing resources and support.

References

- [1] A. Borji. Boosting bottom-up and top-down visual features for saliency estimation. In *IEEE International Conference on Computer Vision and Pattern Recognition*, 2012. 2
- [2] A. Borji and L. Itti. Cat2000: A large scale fixation dataset for boosting saliency research. *CVPR 2015 Workshop on "Future of Datasets"*, 2015. 5, 7, 8
- [3] A. Borji, H. R. Tavakoli, D. N. Sihite, and L. Itti. Analysis of scores, datasets, and models in visual saliency prediction. In *IEEE International Conference on Computer Vision*, 2013. 7
- [4] N. Bruce and J. Tsotsos. Saliency based on information maximization. In *Advances in Neural Information Processing Systems*, pages 155–162, 2005. 2
- [5] Z. Bylinskii, T. Judd, A. Borji, L. Itti, F. Durand, A. Oliva, and A. Torralba. Mit saliency benchmark. <http://saliency.mit.edu/>. 5
- [6] Z. Bylinskii, T. Judd, A. Oliva, A. Torralba, and F. Durand. What do different evaluation metrics tell us about saliency models? *arXiv preprint arXiv:1604.03605*, 2016. 5
- [7] M. Cerf, J. Harel, W. Einhäuser, and C. Koch. Predicting human gaze using low-level saliency combined with face detection. In *Advances in Neural Information Processing Systems*, pages 241–248, 2008. 2
- [8] L.-Q. Chen, X. Xie, X. Fan, W.-Y. Ma, H.-J. Zhang, and H.-Q. Zhou. A visual attention model for adapting images on small displays. *Multimedia systems*, 9(4):353–364, 2003. 1
- [9] J. Chorowski, D. Bahdanau, D. Serdyuk, K. Cho, and Y. Bengio. Attention-based models for speech recognition. In *Neural Information Processing Systems*, 2015. 1
- [10] M. Cornia, L. Baraldi, G. Serra, and R. Cucchiara. A deep multi-level network for saliency prediction. In *International Conference on Pattern Recognition*, 2016. 1, 3, 6, 7, 8
- [11] J. Donahue, L. Anne Hendricks, S. Guadarrama, M. Rohrbach, S. Venugopalan, K. Saenko, and T. Darrell. Long-term recurrent convolutional networks for visual recognition and description. In *IEEE International Conference on Computer Vision and Pattern Recognition*, 2015. 4
- [12] E. Erdem and A. Erdem. Visual saliency estimation by nonlinearly integrating features using region covariances. *Journal of vision*, 13(4):11–11, 2013. 2
- [13] X. Glorot and Y. Bengio. Understanding the difficulty of training deep feedforward neural networks. In *International Conference on Artificial Intelligence and Statistics*, 2010. 6
- [14] S. Goferman, L. Zelnik-Manor, and A. Tal. Context-aware saliency detection. *IEEE Transactions on Pattern Analysis and Machine Intelligence*, 34(10):1915–1926, 2012. 1, 2
- [15] H. Hadizadeh and I. V. Baji. Saliency-aware video compression. *IEEE Transactions on Image Processing*, 23(1):19–33, 2014. 1
- [16] J. Harel, C. Koch, and P. Perona. Graph-based visual saliency. In *Advances in Neural Information Processing Systems*, pages 545–552, 2006. 1, 2, 8
- [17] K. He and J. Sun. Convolutional neural networks at constrained time cost. In *IEEE International Conference on Computer Vision and Pattern Recognition*, 2015. 3
- [18] K. He, X. Zhang, S. Ren, and J. Sun. Deep residual learning for image recognition. In *IEEE International Conference on Computer Vision and Pattern Recognition*, 2016. 2, 3
- [19] S. Hochreiter and J. Schmidhuber. Long short-term memory. *Neural computation*, 9(8):1735–1780, 1997. 4
- [20] X. Huang, C. Shen, X. Boix, and Q. Zhao. SALICON: Reducing the Semantic Gap in Saliency Prediction by Adapting Deep Neural Networks. In *IEEE International Conference on Computer Vision*, 2015. 1, 2, 3, 8
- [21] L. Itti. Visual salience. *Scholarpedia*, 2(9):3327, 2007. 4
- [22] L. Itti, C. Koch, E. Niebur, et al. A model of saliency-based visual attention for rapid scene analysis. *IEEE Transactions on Pattern Analysis and Machine Intelligence*, 20(11):1254–1259, 1998. 2
- [23] S. Jetley, N. Murray, and E. Vig. End-to-end saliency mapping via probability distribution prediction. In *IEEE International Conference on Computer Vision and Pattern Recognition*, 2016. 1, 2, 7, 8
- [24] M. Jiang, S. Huang, J. Duan, and Q. Zhao. Salicon: Saliency in context. In *IEEE International Conference on Computer Vision and Pattern Recognition*, 2015. 2, 5, 6, 7, 8
- [25] T. Judd, F. Durand, and A. Torralba. A benchmark of computational models of saliency to predict human fixations. In *MIT Technical Report*, 2012. 5, 8
- [26] T. Judd, K. Ehinger, F. Durand, and A. Torralba. Learning to predict where humans look. In *IEEE International Conference on Computer Vision*, 2009. 1, 2, 5, 7, 8
- [27] A. Karpathy and L. Fei-Fei. Deep visual-semantic alignments for generating image descriptions. In *IEEE International Conference on Computer Vision and Pattern Recognition*, 2015. 4
- [28] C. Koch and S. Ullman. Shifts in selective visual attention: towards the underlying neural circuitry. In *Matters of intelligence*, pages 115–141. Springer, 1987. 2
- [29] A. Krizhevsky, I. Sutskever, and G. E. Hinton. Imagenet classification with deep convolutional neural networks. In *Advances in Neural Information Processing Systems*, pages 1097–1105, 2012. 2
- [30] S. S. Kruthiventi, K. Ayush, and R. V. Babu. Deepfix: A fully convolutional neural network for predicting human eye fixations. *arXiv preprint arXiv:1510.02927*, 2015. 1, 2, 3, 5, 8
- [31] S. S. Kruthiventi, V. Gudisa, J. H. Dholakiya, and R. Venkatesh Babu. Saliency unified: A deep architecture for simultaneous eye fixation prediction and salient object segmentation. In *IEEE International Conference on Computer Vision and Pattern Recognition*, 2016. 3, 7
- [32] M. Kümmerer, L. Theis, and M. Bethge. Deep Gaze I: Boosting saliency prediction with feature maps trained on ImageNet. *arXiv preprint arXiv:1411.1045*, 2014. 1, 2, 5
- [33] M. Kümmerer, T. S. Wallis, and M. Bethge. Deepgaze ii: Reading fixations from deep features trained on object recognition. *arXiv preprint arXiv:1610.01563*, 2016. 2, 5, 7, 8

- [34] G. Li and Y. Yu. Visual saliency based on multiscale deep features. In *IEEE International Conference on Computer Vision and Pattern Recognition*, 2015. 3
- [35] Z. Li, E. Gavves, M. Jain, and C. G. Snoek. Videolstm convolves, attends and flows for action recognition. *arXiv preprint arXiv:1607.01794*, 2016. 1
- [36] T.-Y. Lin, M. Maire, S. Belongie, J. Hays, P. Perona, D. Ramanan, P. Dollár, and C. L. Zitnick. Microsoft coco: Common objects in context. In *European Conference on Computer Vision*, 2014. 5
- [37] N. Liu, J. Han, D. Zhang, S. Wen, and T. Liu. Predicting eye fixations using convolutional neural networks. In *IEEE International Conference on Computer Vision and Pattern Recognition*, 2015. 2, 8
- [38] V. Mahadevan and N. Vasconcelos. Biologically inspired object tracking using center-surround saliency mechanisms. *IEEE Transactions on Pattern Analysis and Machine Intelligence*, 35(3):541–554, 2013. 1
- [39] N. Murray, M. Vanrell, X. Otazu, and C. A. Parraga. Saliency estimation using a non-parametric low-level vision model. In *IEEE International Conference on Computer Vision and Pattern Recognition*, 2011. 2
- [40] J. Pan, K. McGuinness, S. E., N. O’Connor, and X. Giró-i Nieto. Shallow and Deep Convolutional Networks for Saliency Prediction. In *IEEE International Conference on Computer Vision and Pattern Recognition*, 2016. 2, 3, 7, 8
- [41] R. A. Rensink. The dynamic representation of scenes. *Visual Cognition*, 7(1-3):17–42, 2000. 1
- [42] N. Riche, M. Duvinage, M. Mancas, B. Gosselin, and T. Dutoit. Saliency and human fixations: state-of-the-art and study of comparison metrics. In *IEEE International Conference on Computer Vision*, 2013. 5
- [43] O. Russakovsky, J. Deng, H. Su, J. Krause, S. Satheesh, S. Ma, Z. Huang, A. Karpathy, A. Khosla, M. Bernstein, et al. Imagenet large scale visual recognition challenge. *International Journal of Computer Vision*, 115(3):211–252, 2015. 6
- [44] V. Setlur, S. Takagi, R. Raskar, M. Gleicher, and B. Gooch. Automatic image retargeting. In *International Conference on Mobile and Ubiquitous Multimedia*, 2005. 1
- [45] K. Simonyan and A. Zisserman. Very deep convolutional networks for large-scale image recognition. *CoRR*, abs/1409.1556, 2014. 2
- [46] B. W. Tatler. The central fixation bias in scene viewing: Selecting an optimal viewing position independently of motor biases and image feature distributions. *Journal of vision*, 7(14):4–4, 2007. 5
- [47] T. Tieleman and G. Hinton. Rmsprop: Divide the gradient by a running average of its recent magnitude. *Coursera Course: Neural Networks for Machine Learning*, 2012. 6
- [48] A. M. Treisman and G. Gelade. A feature-integration theory of attention. *Cognitive psychology*, 12(1):97–136, 1980. 2
- [49] P.-H. Tseng, R. Carmi, I. G. Cameron, D. P. Munoz, and L. Itti. Quantifying center bias of observers in free viewing of dynamic natural scenes. *Journal of vision*, 9(7):4–4, 2009. 5
- [50] R. Valenti, N. Sebe, and T. Gevers. Image saliency by isocentric curvedness and color. In *IEEE International Conference on Computer Vision*, 2009. 2
- [51] E. Vig, M. Dorr, and D. Cox. Large-scale optimization of hierarchical features for saliency prediction in natural images. In *IEEE International Conference on Computer Vision and Pattern Recognition*, 2014. 1, 2, 5, 8
- [52] D. Walther, L. Itti, M. Riesenhuber, T. Poggio, and C. Koch. Attentional selection for object recognition a gentle way. In *International Workshop on Biologically Motivated Computer Vision*, pages 472–479. Springer, 2002. 1
- [53] L. Wang, H. Lu, X. Ruan, and M.-H. Yang. Deep networks for saliency detection via local estimation and global search. In *IEEE International Conference on Computer Vision and Pattern Recognition*, 2015. 3
- [54] Q. Wu, P. Wang, C. Shen, A. v. d. Hengel, and A. Dick. Ask me anything: Free-form visual question answering based on knowledge from external sources. In *IEEE International Conference on Computer Vision and Pattern Recognition*, 2016. 4
- [55] K. Xu, J. Ba, R. Kiros, K. Cho, A. Courville, R. Salakhudinov, R. Zemel, and Y. Bengio. Show, attend and tell: Neural image caption generation with visual attention. In *International Conference on Machine Learning*, 2015. 1
- [56] F. Yu and V. Koltun. Multi-scale context aggregation by dilated convolutions. In *International Conference on Learning Representations*, 2016. 3
- [57] D. Zhang, J. Han, C. Li, and J. Wang. Co-saliency detection via looking deep and wide. In *IEEE International Conference on Computer Vision and Pattern Recognition*, 2015. 3
- [58] J. Zhang and S. Sclaroff. Saliency detection: A boolean map approach. In *IEEE International Conference on Computer Vision*, 2013. 1, 2, 8
- [59] Q. Zhao and C. Koch. Learning a saliency map using fixated locations in natural scenes. *Journal of vision*, 11(3):9–9, 2011. 2, 7
- [60] R. Zhao, W. Ouyang, H. Li, and X. Wang. Saliency detection by multi-context deep learning. In *IEEE International Conference on Computer Vision and Pattern Recognition*, 2015. 3